

# Wave-to-wire modelling and hydraulic PTO optimization of a dense point absorber WEC array

Andreas T. Asiikkis<sup>a,b</sup>, Dimokratis G.E. Grigoriadis<sup>b</sup>, Antonis I. Vakis<sup>a,\*</sup>

<sup>a</sup> Computational Mechanical and Materials Engineering, Engineering and Technology Institute Groningen, University of Groningen, Nijenborgh 4, Groningen, 9747, AG, the Netherlands

<sup>b</sup> UCY-CompSci, Department of Mechanical & Manufacturing Engineering, University of Cyprus, 75 Kallipoleos, Nicosia, 1678, Cyprus

## ARTICLE INFO

### Keywords:

Offshore renewable energy  
Wave energy converter array  
Hydraulic power take-off optimization  
Wave-to-wire modeling  
WEC-Sim  
Genetic algorithm

## ABSTRACT

We investigate the hydrodynamic interactions and power extraction efficiency of a dense array of Point Absorber (PA) Wave Energy Converters (WECs) clustered around the fixed pillar of a wind turbine –the Ocean Grazer device– with a standard hydraulic Power Take-Off (PTO) system. Using potential flow theory, a detailed wave-to-wire model is developed in WEC-Sim with four distinct hydraulic PTO designs: i) Multi PTO-with individual hydraulic PTO systems for each buoy, ii) Shared PTO V1-with a unified PTO system for the entire array, iii) Shared PTO V2-with the accumulator volume split into two segments, and iv) Shared PTO V3-with four strategically distributed segments. Key parameters such as the diameter of the hydraulic pistons, volume and pre-charged pressure of the high-pressure accumulators, hydraulic motor displacement and the speed of the electric generator are optimized with a genetic algorithm and a parametric analysis across various sea states. The results highlight that strategically allocating the accumulators across the floaters of a dense WEC array can yield significantly higher power production and should be considered at the early design stages.

## 1. Introduction

The transition to renewable energy sources is a critical step in achieving a carbon-neutral environment. While solar and wind power have advanced significantly, wave energy conversion lags behind despite offering substantial potential, given that oceans cover approximately 70 % of the Earth's surface [1]. Emerging in the late 19th century, Wave Energy Converter (WEC) technologies have a long history, with early concepts dating back to 1799 when the French inventor Pierre-Simon Girard first patented a device to harness wave energy [2]. Since then, WEC technologies have evolved significantly. By the late 19th century, modern WEC concepts began to emerge, and today there are over a thousand designs [3] with an estimated worldwide potential of over 2 TW, of which more than 4 % is feasibly harvestable [4].

The development of WECs is essential to harnessing this potential. Over the past decades, several private companies, start-ups, universities and institutions around the world have dedicated considerable efforts developing various types of WECs. The *European Marine Energy Center* (EMEC, [5]), for example, lists 256 entries of WEC developers. Despite these efforts, according to the International Renewable Energy Agency (IRENA), by the year 2020, only 33 WECs with a combined capacity of

2.3 MW were operational. Most of this capacity hitherto relies on Oscillating Water Column (OWC) technology, with Point Absorber (PA) technology ranking second. Projections suggest that PA technology will dominate future deployments, with a total planned capacity of at least 100 MW [6].

The diversity in PA WEC design is notable, ranging from single body [7–9] to complex multi-body configurations [10–12], and from floating to fully submerged models [13]. These systems can operate in one Degree of Freedom (DOF), such as heave, or up to all six DOFs [14]. A diverse range of PTO systems is employed as well, including hydraulic, mechanical, and Direct-Drive PTO systems. These systems are among the most mature and prevalently used [14]. The present study specifically focuses on the utilization of a hydraulic PTO system.

Optimization techniques, particularly genetic algorithms [15], have been employed to enhance WEC performance due to their ability to effectively search large solution sets and find optimal configurations for complex systems [16,17]. Other optimization techniques have also been widely used, such as metaheuristic [18,19], particle swarm [20,21] and others [15]. For instance Ref. [22], employed several optimization algorithms to optimize the piston area and the volumes and pre-charged pressure of the accumulators with the results indicating a 304 %

\* Corresponding author.

E-mail addresses: [a.asiikkis@rug.nl](mailto:a.asiikkis@rug.nl) (A.T. Asiikkis), [grigoria@ucy.ac.cy](mailto:grigoria@ucy.ac.cy) (D.G.E. Grigoriadis), [a.vakis@rug.nl](mailto:a.vakis@rug.nl) (A.I. Vakis).

increase in power production. In Ref. [23], the displacement of the hydraulic motor, along with the shaft inertia and damping coefficients, were optimized for several wave conditions ensuring the highest efficiency possible. Similar studies focusing on the optimization of hydraulic PTO systems include [24–27].

Furthermore, recent advancements have emphasized the strategic placement of multiple PA WECs in arrays to maximize energy extraction and minimize the sea surface required [28]. The Ocean Grazer dense WEC array represents a significant advancement in harnessing wave energy due to its novel dense configuration which can further increase power extracted per area as long as the hydrodynamic interactions within each array can be properly predicted and designed. Initially, the concept involved a floater blanket composed of interconnected floaters [29]. Subsequently, this model evolved with the floaters having some space in between [30]. A more recent investigation has shed light on how the adaptability within the PTO system can enhance power extraction by focusing on a unique PTO consisting of three pistons with varying sizes, thus providing seven different pumping combinations and thereby enhancing the system's adaptability and efficiency [30]. In this work, we focus on an updated version of the Ocean Grazer (v. 4.0) that uses standardized hydraulic PTO components and decouples energy generation from storage.

Several studies employed optimization and control techniques to maximize power extraction by optimizing key components of a hydraulic PTO. To the best of the authors' knowledge, no research has examined how the distribution of accumulator volume affects power performance, specifically when the total volume is held constant but divided among the floaters of a WEC array using different strategies. The importance of this work lies in addressing this gap in the literature by assessing various accumulator placements within the dense WEC array of the Ocean Grazer 4.0, following optimization of the PTO system parameters under several regular wave conditions. Furthermore, this is the first study to incorporate a standard hydraulic PTO in the Ocean Grazer design that allows for bidirectional energy harvesting.

The structure of this paper is organized as follows. We start with the design of the Ocean Grazer 4.0 WEC array and the PTO system, laying the foundation for our investigation. This is followed by a brief presentation of the mathematical formulation and the numerical model. We then delve into the convergence analysis of the spatial and temporal discretization parameters, ensuring the robustness and accuracy of our numerical model. Then the optimization results of four distinct PTO designs are revealed under various regular wave conditions. A comprehensive and critical discussion then synthesizes these results, drawing attention to the key findings of this study, which show that utilizing shared PTO configurations can substantially increase the power extraction under a wide range of wave conditions.

## 2. WEC array and PTO dynamics

### 2.1. Ocean Grazer 4.0 concept

This study is inspired by the innovative design of the Ocean Grazer 3.0 [31], particularly its dense array of PA WECs clustered around the fixed pillar of a wind turbine. The original Ocean Grazer concept is integrated with an offshore energy storage system known as the Ocean Battery [32], which utilizes the hydrostatic pressure at the seabed to store significant amounts of energy in bladders filled with pressurized fluid. However, the focus of our study diverges from this approach as we aim to investigate the performance of dense PA WEC arrays equipped with standard hydraulic PTO systems that extract energy in both the up- and downstroke using oil as the working fluid. By decoupling from the Ocean Battery concept, we assess traditional hydraulic PTO configurations within the dense WEC array framework. Our primary objective is the hydrodynamic modelling of the heaving PA WECs and the optimization of the PTO system for electricity generation. Four distinct hydraulic PTO designs are under consideration to explore their

effectiveness and optimization in a dense WEC array setup.

### 2.2. Mathematical formulation

The open-source computational tools Capytaine [33] and Wave Energy Converter Simulator (WEC-Sim) [34] were adopted for developing the wave-to-wire model of Ocean Grazer 4.0. Capytaine focuses on determining the hydrodynamic coefficients of the floaters in the frequency domain. These are then used as input parameters for WEC-Sim, which handles the complex multi-body dynamics of the system using the Cummins equation. Herein, the main features of these tools will be presented along with the implemented assumptions and a brief description of the mathematical modelling. For more details, the reader is referred to the theory manuals and publications of Capytaine [35] and WEC-Sim [36,37].

#### 2.2.1. Capytaine – Mathematical formulation

Capytaine is a Python-developed package based on the Nemoh Boundary Element Method (BEM) [38]. It is based on potential flow theory, which assumes that the fluid is inviscid and the flow is incompressible and irrotational. These assumptions, albeit simplifying in nature, can lead to an omission of certain viscous effects and limit the predictive accuracy. Nevertheless, despite these assumptions, in the initial design stages of new WEC systems, the BEM approach provides a valuable balance between computational efficiency and fidelity. Capytaine's OpenMP parallelization capabilities make it an ideal choice for this study due to the need for high computational efficiency, given the task of analyzing the dynamics of a large array of floaters, which inherently involves substantial computational demands.

By expressing the velocity of the water as a velocity potential  $\varphi(x,y,z,t)$ , the water velocity field can be described as  $\vec{u} = \nabla\varphi$ . Substituting this into the incompressibility ( $\nabla \cdot \vec{u} = 0$ ) and irrotationality ( $\nabla \times \vec{u} = 0$ ) conditions results in a Laplace equation for the velocity potential:

$$\nabla^2\varphi = 0. \quad (1)$$

By considering the linear wave theory, the velocity potential can be expressed in the frequency domain by the complex amplitude  $\Phi$ , and the unit amplitude  $e^{i\omega t}$  as:

$$\varphi(x,y,z,t) = \text{Re}(\Phi e^{-i\omega t}) \quad (2)$$

and by moving from the time domain to the frequency domain, eq. (1) becomes:

$$\nabla^2\Phi = 0 \quad (3)$$

The boundary conditions of the problem become:

1. Along the free surface ( $z = 0$ ):

$$g \frac{\partial\Phi}{\partial z} - \omega^2\Phi = 0 \quad (4)$$

2. At the seabed ( $z = -h$ ), where  $h$  is the water depth:

$$\frac{\partial\Phi}{\partial z} = 0 \quad (5)$$

3. The velocity  $\vec{u}$  on the surface  $S$  of the bodies:

$$\nabla\Phi \cdot \vec{n} = \vec{u} \cdot \vec{n} \quad (6)$$

where  $\vec{n}$  is the normal vector at the surface.

The boundary value problem for wave-body interaction involves

solving Laplace’s equation for the velocity potential  $\varphi$  subject to the boundary conditions at the free surface, the seabed, and along the body surface. The solution to this problem determines the pressure field around the body and, consequently, the forces acting on the body. For further details and a comprehensive overview of the equations involved, the reader is referred to the Capytaine theory manual [35].

### 2.2.2. WEC-Sim – Mathematical formulation

**2.2.2.1. Kinematics of floating bodies.** WEC-Sim [34] is an advanced open-source design tool for WECs, collaboratively developed by the National Renewable Energy Laboratory (NREL) and Sandia National Laboratories. It provides mid-fidelity simulations based on linear wave theory, by solving the equation of motion for floating bodies across all six DOFs. Developed within the MATLAB/SIMULINK environment, it can simulate a wide range of WEC components in the time domain. This includes, but is not limited to, hydrodynamic bodies, constraints and PTOs. When compared to high fidelity computationally intensive approaches like Computational Fluid Dynamics (CFD), WEC-Sim has a relatively low computational cost. Especially for optimization purposes, this enables the application of genetic algorithms, where many simulations must be completed before reaching optimized configurations.

WEC-Sim solves the kinematics of floating bodies by considering several hydrodynamic forces. The equation of motion for a floating body reads,

$$m\ddot{X} = F_{exc}(t) + F_{rad}(t) + F_B(t) + F_{md}(t) + F_v(t) + F_{me}(t) + F_{pto}(t) + F_m(t) \quad (7)$$

where,  $F_{exc}$  is the wave excitation force,  $F_{rad}$  is the radiation force and  $F_B$  is the buoyancy force, all calculated using the Capytaine code.  $F_{exc}$  is calculated based on two components, namely, the Froude-Krylov force and the diffraction force.  $F_{rad}$  is calculated by the sum of the added mass and radiation damping terms by  $F_{rad}(t) = -A(\omega)\ddot{X} - B(\omega)\dot{X}$ , where  $X$  is

the displacement of the floating body,  $A$  is the added mass and  $B$  is the radiation damping for a given wave frequency  $\omega$ .  $F_{md}(t)$  represents the mean drift force, a second-order force with minimal variation over time.  $F_v(t)$  is the viscous damping force caused by the viscous effects of the fluid and  $F_{me}$  is the Morison Element force, which accounts for the drag and inertia forces on slender bodies in oscillatory flows. These terms are neglected in this work because WEC-Sim uses linear wave theory to model WECs. These nonlinear forces are typically included when buoyancy effects or viscous forces are significant. However, determining accurate coefficients for these terms requires either experimental data or detailed CFD simulations, which are beyond the scope of this work, since the main objective is the optimization of the PTO under several wave conditions, which requires computational efficiency.  $F_{pto}$  is the force acting on the body from the hydraulic PTO system and  $F_m$  is the mooring force which is not accounted for here due to the absence of moorings as such.

**2.2.2.2. PTO force and dynamics.** The PTO system in WEC-Sim is modeled through Simulink blocks retrieved from the PTO-Sim library [37]. Hydraulic PTOs with oil as the working fluid were used in this work, which are discussed later and shown in Fig. 2. The heave motion of the floaters drives the vertical motion of double-acting hydraulic pistons that pump oil due to the pressure developed in the piston chambers. The pressure difference between the two chamber A and B exerts the PTO force on the buoy,  $F_{pto}$ , defined as:

$$F_{PTO} = (p_A - p_B)A_p \quad (8)$$

where  $p_A$  and  $p_B$  denote the pressure developed in the chambers A and B respectively, due to the motion of the buoy, and  $A_p$  is the area of the hydraulic piston.

The power produced by the PTO is calculated through the following equation:

$$P_{PTO} = -F_{PTO}\dot{X}. \quad (9)$$

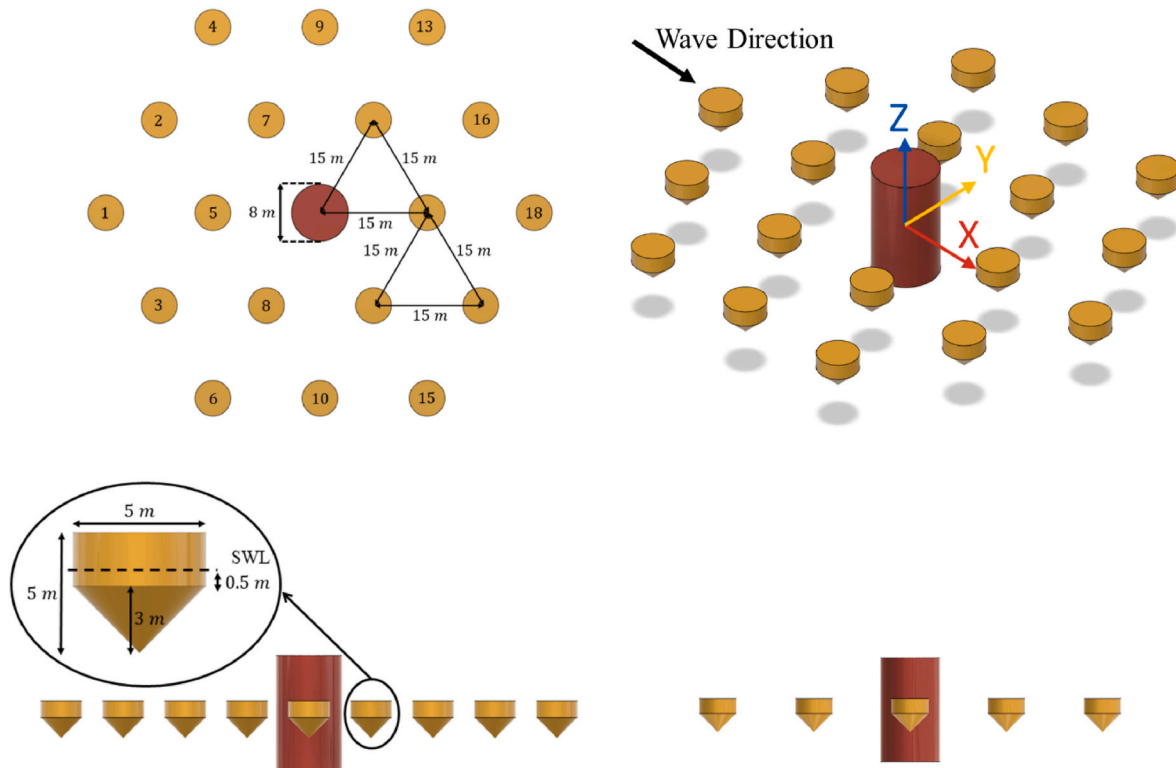


Fig. 1. Orthographic projection and basic dimensions of the Ocean Grazer WEC array, with 18 buoys configured in a honeycomb layout around the monopile of a wind turbine.

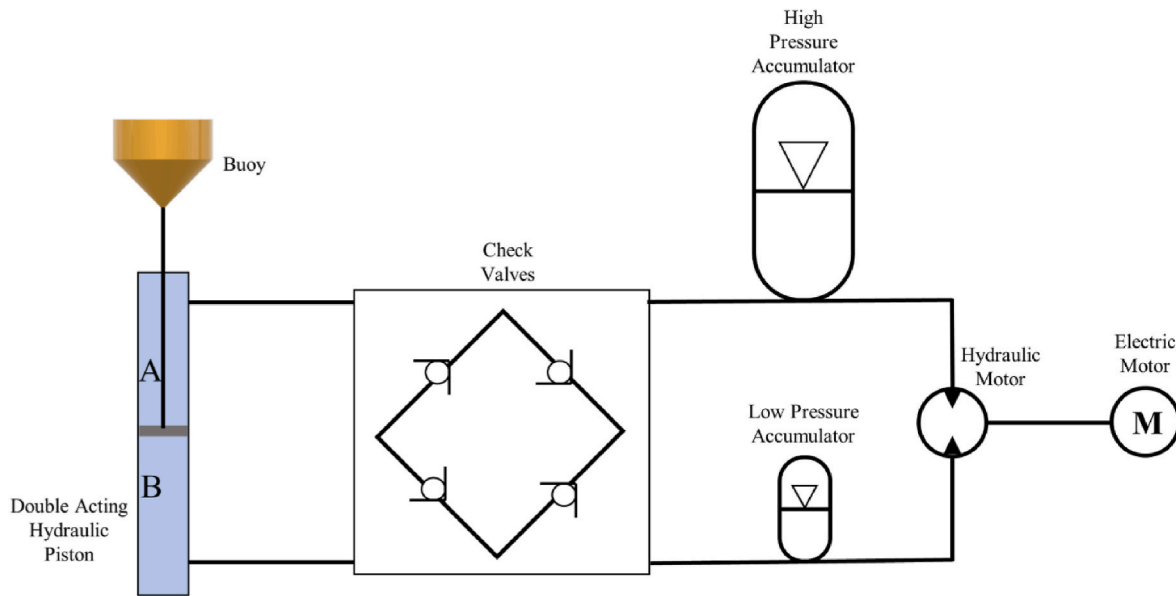


Fig. 2. Multi-PTO design: an independent PTO system assigned for each floater of the Ocean Grazer WEC array. Each floater is connected to its own PTO system via a taut cable.

For more information about the mathematical formulation of the PTO-Sim library, the reader is referred to the relevant publication [37].

2.2.3. Genetic algorithm

Genetic Algorithms (GAs) are a class of evolutionary algorithms that mimic the process of natural selection. These algorithms are used to find optimal or near-optimal solutions to complex problems, which might be difficult to solve using traditional methods. While our model is based on linear wave theory, the design parameters of the hydraulic PTO system introduce non-linearities and a complex, multidimensional optimization space. Therefore, in this work, a genetic algorithm was used utilizing the Global Optimization Toolbox of MATLAB (Version R2023b, The MathWorks, Inc.), with the optimization parameters (i.e., genomes) depicted in Table 1 and the generated power being the fitness function.

The iterative process of the GA allows it to progressively improve the solutions, converging towards the optimal settings for the hydraulic PTO parameters. By using GAs, the study efficiently navigates the complex, multidimensional search space to identify the most effective configurations for maximizing power extraction under various wave conditions. The steps of how the GA works can be found in Ref. [39].

3. Numerical model set-up

3.1. WEC-array

The Ocean Grazer concept’s WEC array, as depicted in Fig. 1, features 18 circular buoys arranged in an efficient honeycomb pattern. Centrally located within this configuration is a wind turbine. Each buoy, cylindrical in form, measures 5 meters in diameter and 2 meters in height. Below each cylinder, a conical extension adds an additional 3

Table 1 Investigated parameters and fitness function for the genetic algorithm.

Investigated Parameters	Fitness Function
Piston diameter $D_p$	Generated Electrical Power
Initial volume of the gas in the high-pressure accumulator $V_{10}$ ,	
Pre-charge pressure of the accumulator $p_{10}$ ,	
Hydraulic Motor Displacement $D_h$	
Generator Speed $n_g$	

meters to the buoy’s height. To ensure optimal functioning, a spacing of 15 meters is maintained between each buoy. The geometry parameters, including diameter, density, mass and inertia of the buoys are shown in Table 2.

3.2. PTO designs

3.2.1. Multi PTO design (individual PTO for each floater)

In the first PTO design, shown in Fig. 2, each floater is independently connected to its own PTO system via a stiff taut cable. This configuration comprises a hydraulic piston that converts mechanical energy from wave motion into hydraulic energy. Each piston is integrated with a system of four rectifying valves ensuring unidirectional hydraulic flow. The rectified flow is then directed into two accumulators—one high-pressure and one low-pressure—to temporarily store hydraulic energy and smoothen power generation. This stored hydraulic energy is subsequently converted back into mechanical energy by a hydraulic motor, which drives an electrical generator to produce electricity. The independent PTO system for each floater allows for localized energy conversion, minimizing the interference between floaters and maximizing individual energy capture efficiency.

3.2.2. Shared PTO V1 design (single global PTO system)

In the second design considered, a centralized approach is implemented where all floaters share a single global PTO system as illustrated in Fig. 3. Similar to the Multi PTO design of the previous section, each floater has its own hydraulic piston and rectifying valves. However, in this configuration, all floaters are connected to a common set of high- and low-pressure accumulators. These accumulators have a volume

Table 2 Parameters of a single buoy in the Ocean Grazer WEC array, including the diameter, density, mass, and moments of inertia about the x, y, and z axes.

Parameters	Value	Unit
Diameter ( $D$ )	5	$m$
Density ( $\rho$ )	469.4	$Kg/m^3$
Mass ( $m$ )	26111	$Kg$
Inertia	x-axis ( $I_{xx}$ )	974400
	y-axis ( $I_{yy}$ )	974400
	z-axis ( $I_{zz}$ )	1204000

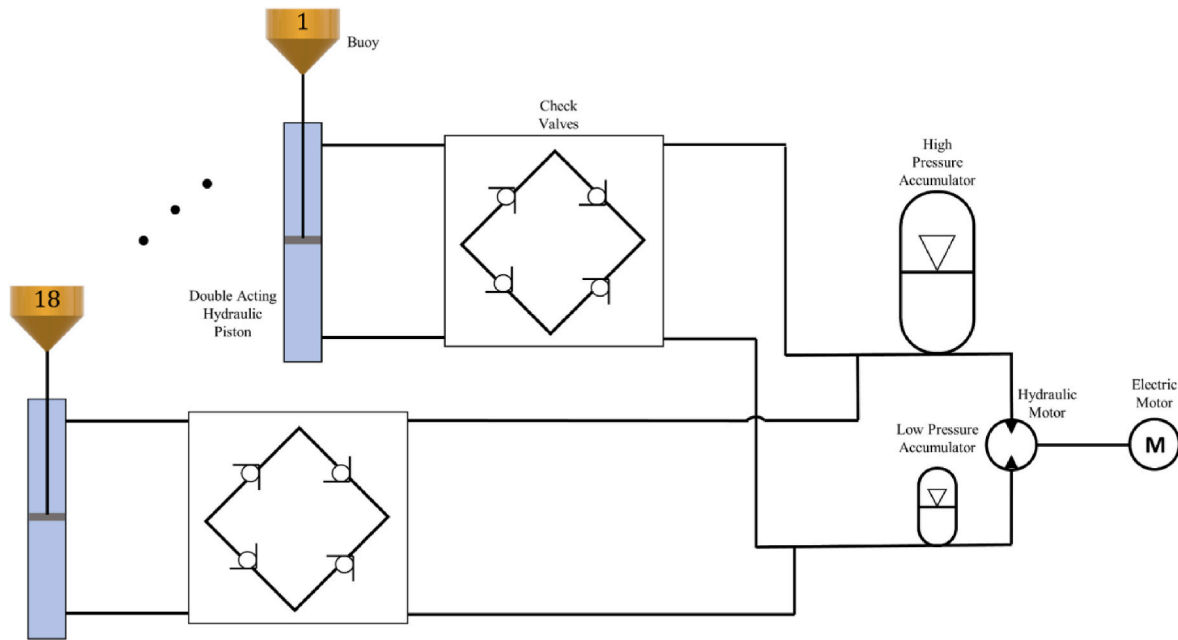


Fig. 3. Shared-PTO design of the Ocean Grazer WEC array. Each WEC unit comprising of a buoy, a hydraulic piston and check valves, is connected to a centralized system of accumulators, hydraulic motor and electric motor.

equivalent to the sum of the individual volumes used in the Multi PTO design. The centralized accumulators drive a single hydraulic motor coupled with an electrical generator. Just as the Ocean Grazer 3.0 [40] utilizes the Ocean Battery for a centralized energy storage solution, the Ocean Grazer 4.0 employs a shared accumulator system to simplify the overall system by centralizing the energy conversion process, potentially reducing mechanical complexity and maintenance requirements while facilitating coordinated energy storage and conversion.

3.2.3. Additional shared PTO designs

To explore the impact of accumulator volume distribution on PTO system performance, two additional designs were developed to examine the collective energy capture of the array, as shown in Fig. 4. These designs were strategically chosen to consider only one wave direction (from left to right in the figure), thereby simplifying the wave dynamics and clarifying PTO system’s behavior.

3.2.3.1. Third design: Splitting accumulators based on position relative to the pillar (shared PTO V2).

This configuration divides the array into two sections: floaters in front of the central pillar (floaters 1–10) and those behind (floaters 11–18), each sharing its own set of high- and low-pressure accumulators. This strategic split aims to optimize the

collective energy capture and storage within each section by grouping floaters that are influenced by similar wave conditions and interactions from the central pillar.

3.2.3.2. Fourth design: synchronization-based grouping (shared PTO V3).

In this design, floaters are grouped based on their phase synchronization with incoming waves, sharing accumulators within these groups. This approach manages phase differences reducing destructive interference and enhancing energy conversion efficiency.

All the above volume distribution strategies are illustrated in Fig. 4. It should be noted that the omnidirectionality of the array can still be achieved in the shared versions (V2 and V3) by controlling which array members connect to which accumulators during operation. These innovative PTO designs comprehensively explore how strategic accumulator volume distribution influences the performance of such dense WEC arrays, addressing wave interactions and phase synchronization challenges to optimize energy conversion in hybrid platforms like the Ocean Grazer.

Uniformity in parameter settings is crucial for the optimization process. For each wave scenario tested, the diameter of the hydraulic pistons is uniformly optimized across all pistons, though this optimized value may vary between different wave conditions. This approach is also

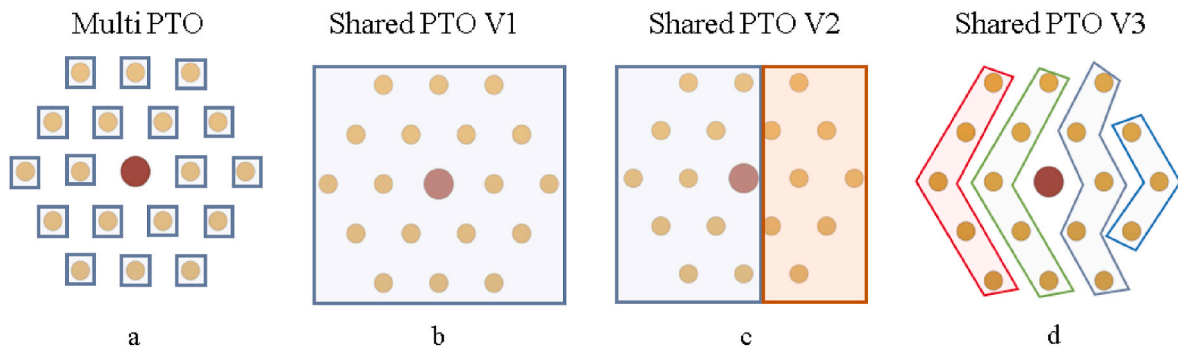


Fig. 4. Schematic representation of the four PTO designs considered for the Ocean Grazer WEC array. a) Multi PTO: Each floater has an independent PTO system. b) Shared PTO V1: The entire array shares a single set of accumulators. c) Shared PTO V2: The array is split into two sections, each with its own set of accumulators. d) Shared PTO V3: Floaters are grouped based on their phase synchronization with incoming waves (from left to right), each group sharing accumulators.

applied to the hydraulic motor displacement and generator speed. However, there are distinctions in the implementation between the two systems. While the Shared PTO V1 system utilizes a single hydraulic motor and generator, the Multi PTO system employs multiple units of each, with uniform settings across a given wave condition.

Furthermore, the total volume of accumulators remains constant, even when split into smaller units. The study aims to determine whether distributing the accumulator's volume across multiple units within the array affects power output. By testing different configurations of accumulator distribution (Fig. 4), we aim to pinpoint the most effective allocation of accumulator volume that maximizes power performance across all tested wave conditions. This systematic approach helps in identifying the optimal number of accumulators and their distribution to achieve the best efficiency and reliability in wave energy conversion across the entire WEC array. In our current model, we only consider a single wave direction to simplify the analysis and focus on evaluating whether the accumulator distribution can improve power generation.

### 3.3. Characterization of the PTOs

The design and development of PTO systems for WECs present unique challenges due to the evolving nature of the technology and the variety of WEC designs, each requiring customized PTO solutions [41]. This complexity is further increased by the nonlinear interactions among PTO components and the irregular wave excitation forces they must process. To address these challenges, we adopted a systematic methodology for selecting the parameters for the PTO systems under study.

#### 1. Literature Review:

A comprehensive review of existing literature was conducted to establish a range of PTO parameter values. This review included various studies on hydraulic PTO systems, highlighting typical parameter configurations and performance outcomes. The goal was to identify a baseline for parameter values that are commonly used and validated in the field.

#### 2. Manufacturer Specifications:

To refine the parameters for the specific PTO designs under consideration, we analyzed data from the manufacturer Parker Hannifin [42]. This manufacturer provides detailed specifications for hydraulic components, ensuring that the parameter values chosen are feasible and applicable.

Table 3 summarizes the required parameters for modeling a hydraulic PTO system within the PTO-Sim module of WEC-Sim. These parameters are contrasted with configurations from seven distinct numerical models documented in peer-reviewed journals and conference publications. This structured approach ensures that the parameters used in the modeling of the PTO systems are both scientifically grounded and practically feasible.

Table 3 highlights the diversity and complexity of parameter values, underscoring the necessity of employing optimization techniques to achieve the best possible performance. This methodology not only facilitates the early design phase but also ensures a comprehensive understanding of how each parameter influences the overall system efficiency. Utilizing tools like WEC-Sim allows for the simulation of numerous configurations within a reasonable timeframe, providing a solid foundation for iterative optimization and further refinement of the PTO systems before developing an experimental system.

#### 3.4. Methodology for assessing the PTO parameters

To properly assess the influence of the parameters of the PTO system, a parametric analysis approach is used. A default set of parameters was set based on the manufacturer's values given in Table 3. Several sets of

**Table 3**

Range of parameters used to model the hydraulic PTO system within the PTO-Sim module of WEC-Sim. This table presents a parametric range from seven distinct numerical models documented in the literature and manufacturer specifications. The last column shows the values considered here.

Parameter	Units	Literature [22,23,25–27, 43,44]	Manufacturer range	Simulation values
Buoy mass	Kg	858 – 727000	–	26111
Diameter of piston	m	0.025 – 0.203	0.032 – 0.125 [45]	0.0798 – 0.125
Area of piston	m <sup>2</sup>	0.00051 – 0.032	0.000805 – 0.01227	0.005 – 0.01227
Stroke Limit	m	0.3 – 5	0 – 2 [45]	5
Piston Initial pressure	MPa	0 – 20.7	20 (max. operating press.) [45]	20
HPA Pre-Charge Pressure	MPa	0 – 500	33 – 69 (max. operating press.) [46]	15 – 69
HPA Volume	m <sup>3</sup>	0.0002 – 10	0.00017 – 0.051 [46]	0.01 – 0.051
LPA Pre-Charge Pressure	MPa	0 – 300	4 (max. operating press.) [47]	4
LPA Volume	m <sup>3</sup>	0 – 8	0.01 [47]	0.01
Hydraulic Motor Displacement	$\frac{cc}{rev}$	19 – 23034	75 – 9000 [48]	75 – 500
Electric Generator Resistance (Ra)	Ohm	0.483 – 8	0.0167 [49]	0.0167
Electric Generator (Ke)	$\frac{V}{rad/s}$	7.186	1.85 [49]	1.85
Electric Generator Inertia (Jem)	$Kg\ m^2$	0.0036 – 2	0.56 [49]	0.56
Electric Generator (bshaft)	$\frac{Nm}{rad/s}$	0.024 – 9.5	–	0.01
Generator Speed	rpm	200 – 500	1660 – 7000 [49]	1660 – 7000

simulations were performed by changing one parameter while all the others were held constant, for five different regular wave conditions and wave periods. The aim was to understand how each parameter affects the power extracted by the array and examine whether a linear or nonlinear relationship exists between the PTO parameters and power extraction.

After the parametric analysis, the most critical parameters were selected for optimization through a genetic algorithm. The workflow of the optimization process is illustrated in Fig. 5. Initially, the WEC geometry is used in Capytaine to calculate the hydrodynamic coefficients. The resulting data are given as input in WEC-Sim after a pre-processing using the BEMIO code of WEC-Sim. The genetic algorithm implemented through MATLAB's Global Optimization Toolbox, iteratively adjusts the selected PTO parameters, aiming to maximize power extraction. The simulation results are then processed to assess the convergence of the genetic algorithm and to generate power matrices that visualize the performance of different PTO configurations.

#### 3.5. Numerical setup and sensitivity analysis

##### 3.5.1. Capytaine setup and sensitivity analysis

To properly configure the hydrodynamic model in Capytaine, a set of additional inputs parameters are required, as listed in Table 4. The primary input is the geometry of the object for which hydrodynamic coefficients are to be calculated. The geometry is defined by centroids and vertices of the mesh panels. The discretization level of the mesh influences the precision of the results and must therefore be examined to ensure convergence. The process of analyzing the mesh convergence includes a quantitative and qualitative assessment, comparing the

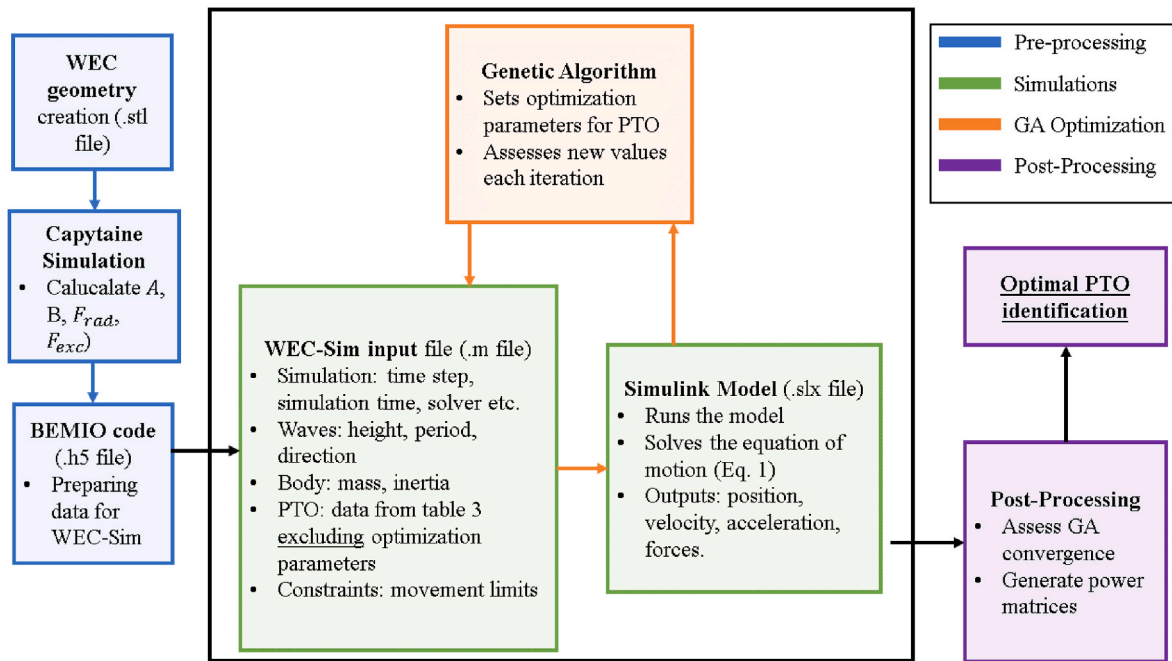


Fig. 5. Workflow for the optimization of the PTO system. The process includes the geometry creation, hydrodynamic coefficients calculation, parameter setting in WEC-Sim, genetic algorithm optimization, and post-processing to identify the optimal PTO configuration.

Table 4

Input parameters used for the hydrodynamic model of the Capytaine simulations.

Parameters	Values	Units
Wave Heading	0	$^{\circ}$
Wave Frequency	0.4 : 0.095 : 8	rad/s
Depth	60	m
Density	1000	Kg/m <sup>3</sup>
Number of panels	1366 1842 2582	[ - ]

calculated values of added mass, radiation damping, and wave excitation forces across various panel sizes.

Fig. 6 displays the non-dimensional added mass ( $\bar{A} = A(\omega)/\rho$ ) and radiation damping ( $\bar{B} = B(\omega)/(\rho\omega)$ ) results for the 1<sup>st</sup> and 18<sup>th</sup> floaters in the array, which coincide with the first and last along the wave propagation direction, respectively, as shown in Fig. 1. The outcomes for both floaters appear similar, aligning with expectations. However, subtle variations between them are present, though not visually discernible in figures. A comparative analysis of mesh quality - transitioning from coarse to medium, and from medium to fine - suggests that results progressively align more closely with those of the fine mesh, as illustrated in the zoomed-in section.

Given the visual ambiguity in mesh differences, a quantitative method was employed to calculate the percentage change from coarse to medium, and from medium to fine, for each frequency. The average of these percentage changes is presented in Table 5. For both floaters, the percentage variation in added mass across mesh pairings is notably minimal. In contrast, the changes in radiation damping are slightly more pronounced, yet still modest enough to deem the results as having converged. This pattern can be primarily attributed to the significant fluctuation of radiation damping values across the frequency spectrum. The fine mesh was selected since Capytaine needs to run only once and its computational cost does not affect the subsequent WEC-Sim simulations.

### 3.5.2. WEC-Sim setup and sensitivity analysis

This section outlines the parameters for the WEC-Sim simulations, incorporating a sensitivity analysis on time-step selection. The analysis focused on three time-steps ( $\Delta t = 0.001, 0.0005, 0.0001$  s), with the extracted electrical power serving as a critical metric due to its relevance in assessing the system's energy conversion efficiency. The selection of the largest time-step (0.001 s) was based on achieving a balance between accuracy and computational efficiency, since minor differences were observed among the time-steps as illustrated in Fig. 7. Computational times for each scenario are provided in Table 6 highlighting the optimized time-step's benefit in reducing computational load without significantly compromising result accuracy.

The quantitative sensitivity analysis, provided in Table 7, demonstrates that the percentage differences in both the heave response and power generation between time steps were very small. Therefore, the time step of 0.001 s was selected to significantly reduce computational cost, by more than 89 %, while maintaining accuracy, since the percentage difference between the smallest and largest time steps was just 1.2 % for the heave response and only 0.031 % for the power generated.

## 4. Results and discussion

### 4.1. Parametric analysis of PTO parameters

In the preliminary phase of this research, the performance of two hydraulic PTO systems was investigated under five distinct regular wave scenarios, each with the same wave height but different wave period. By altering only the wave period, a consistent framework was formulated within which we could assess the influence of variables on system behavior. As mentioned, in Table 1, the parameters in question are:

1. Diameter of the hydraulic pistons  $D_p$ ,
2. Initial volume of the gas in the high-pressure accumulator  $V_{i0}$ ,
3. Pre-charge pressure of the accumulator  $p_{i0}$ ,
4. Hydraulic motor displacement  $D_h$ ,
5. Reference speed of the electric generator  $n_g$ .

The insights gained from this investigation formed the subsequent

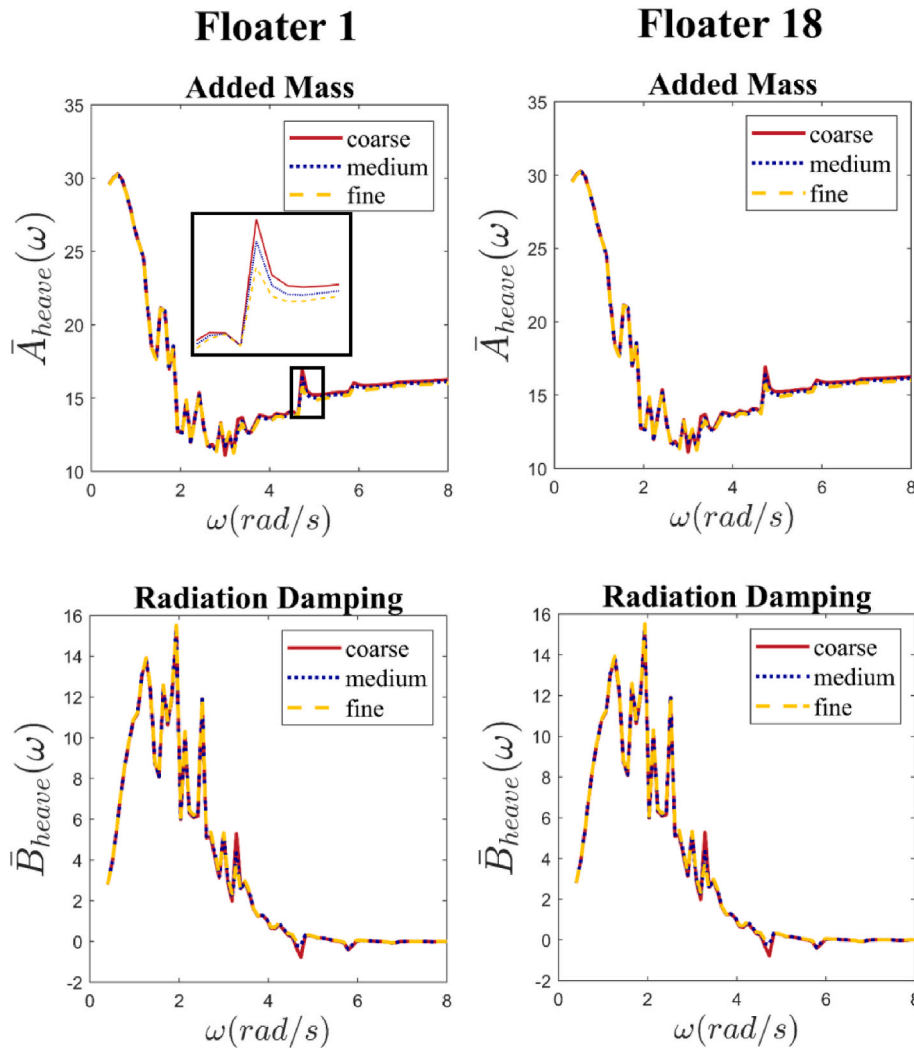


Fig. 6. Effect of mesh resolution on the non-dimensional added mass and radiation damping coefficients for Floater 1 and 18, predicted by Capitaine. The graphs show the heave mode coefficients as a function of wave frequency ( $\omega$ ) for three different mesh resolutions.

Table 5

Effect of grid refinement on the percentage change [%] in added mass and radiation damping coefficients for Floater 1 and Floater 18, predicted by Capitaine.

Meshes	Added Mass Percentage Change [%]		Radiation Damping Percentage Change [%]	
	Floater 1	Floater 18	Floater 1	Floater 18
	Coarse to Medium	0.75 %	0.75 %	1.89 %
Medium to Fine	0.63 %	0.64 %	- 3.49 %	- 3.49 %

optimization stage, wherein a genetic algorithm was applied to refine these parameters across a broader range of wave conditions. The following results provide a comprehensive understanding of how each PTO parameter affects the performance of the whole array.

#### 4.1.1. Diameter of the hydraulic pistons

Fig. 8 presents the influence of piston diameter on the actual power generated for both Multi and Shared PTO V1 systems for various wave conditions. It is evident that there is a nonlinear relationship between the piston diameter and power output.

For the Multi PTO system, the maximum power output is observed at different piston diameters for each wave period. At a wave period of 6 seconds, an optimal piston diameter of 9.6 cm yields 1024 KW of power.

As the wave period increases to 8 seconds, a larger diameter is optimal and the trend continues with increasing wave periods. The same diameter is optimal for the wave periods of 12 and 14 seconds because the optimal diameter for these conditions is the highest value possible indicating that a larger diameter would be needed for optimal power extraction at a wave period of 14 seconds.

The Shared PTO system follows a similar pattern, with each wave period favoring a different piston diameter for optimal power production, albeit at smaller diameters compared to the Multi PTO system.

This behavior underscores a critical fact: the optimal diameter of the hydraulic piston is not a static parameter but rather one that varies in accordance with the sea state. Furthermore, the results indicate that the Multi PTO system requires larger piston diameters for increased wave periods, whereas the Shared PTO system maintains efficiency with smaller diameters, possibly due to synergistic effects in the shared accumulator design. The nonlinear characteristics of the curves in the figure reaffirm the complexity of the relationship between piston diameter and power production, highlighting the necessity for a tailored approach to PTO design to harness the maximum energy from waves.

#### 4.1.2. Initial volume and pre-charge pressure in the high-pressure accumulator

Fig. 9 shows how the initial volume in the high-pressure accumulator influences power production. It is observed that, for the Shared PTO

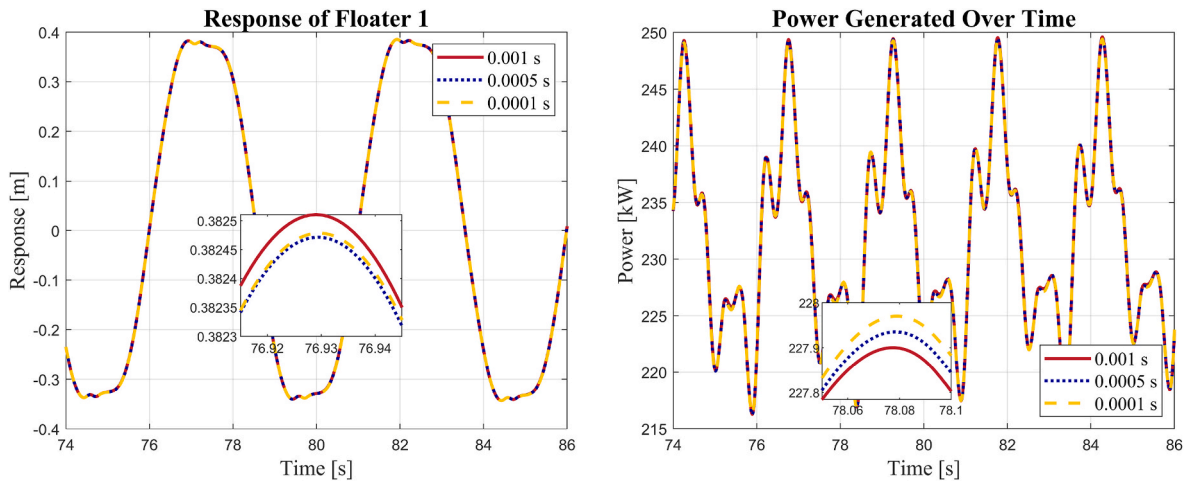


Fig. 7. Effect of temporal resolution in WEC-Sim simulations. The response of Floater 1 (left figure) and the power generated over time (right figure) simulated with three different time-steps.

Table 6

Computational times in wall clock seconds for numerical simulations using WEC-Sim with different time-steps.

Time Step $\Delta t$ [s]	Computational Cost [s]
0.001	390
0.0005	737
0.0001	3032

Table 7

Sensitivity analysis results comparing heave response, power generation, and computational cost savings for different time steps in the WEC-Sim simulations.

Time-steps [s]	Heave Response Percentage Change [%]	Power Generation Percentage Change [%]	Computational cost savings
0.001 to 0.0005	0.77 %	0.020 %	89%
0.0005 to 0.0001	0.29 %	0.012 %	311%
0.001 to 0.0001	1.2 %	0.031 %	677%

system, the relationship between the initial gas volume and the power extracted is relatively linear, indicating a stable enhancement in power as the volume increases, irrespective of the wave conditions. The trend suggests that larger volumes consistently yield higher power outputs, an observation that remains true across all tested wave periods. This tendency is mirrored in the Multi PTO system, albeit with a slightly more variable response. The increase in power is not as linearly correlated with the volume as it is for the shared PTO system, yet the general observation that greater volumes facilitate higher power production still holds. Additionally, for both PTO configurations, it is noticeable that shorter wave periods favor increased power production.

The pre-charge pressure within the high-pressure accumulator reveals a trend similar to that of the initial gas volume, as illustrated in Fig. 10. Across varying wave conditions, it is noted that increasing the pre-charge pressure correlates with an increment in power output for both the multi and shared PTO systems.

The consistent increase in power with larger values of these parameters suggest that the initial gas volume and pre-charge pressure are not a limiting factor in the PTO’s performance. These parameters exhibit a clear-cut behavior: maximizing their value yields the best results regardless of the wave conditions. Given this straightforward relationship, it is concluded that these PTO parameters do not require

optimization through the genetic algorithm. Instead, setting these parameters to their maximum feasible value simplifies the design process and ensures optimal power production.

#### 4.1.3. Hydraulic motor displacement

The relationship between hydraulic motor displacement and power produced by the two PTO systems offers insightful trends regarding their operational efficiencies as shown in Fig. 11. In both multi and shared PTOs, the optimum hydraulic motor displacement exhibits a decrease as the wave period increases. This phenomenon could be attributed to the dynamic interaction between wave period and the responsiveness of the hydraulic system. Longer wave periods result in slower buoy movements, thereby requiring less fluid displacement for optimal energy transfer. Conversely, shorter wave periods, with more rapid oscillations, necessitate greater fluid displacement to capture the energy efficiently. This inverse relationship indicates that the hydraulic system’s capacity is closely matched to the energy input frequency, which is critical for achieving maximum energy extraction.

The power-hydraulic displacement curves further reveal a clear peak, indicating an optimal displacement value for each wave condition. A deviation from this optimum can lead to a significant drop in power generation, underscoring the sensitivity of this parameter. Consequently, hydraulic displacement is considered a crucial parameter in the PTO design that requires precise optimization for different wave conditions.

#### 4.1.4. Reference speed of the electric generator

Similarly to the hydraulic displacement, the optimal generator speed within the PTO systems exhibits a direct relationship with the frequency of incoming waves. It is observed in Fig. 12 that as the wave period increases, signifying slower oscillatory motion of the buoys, the generator speed that yields maximum power decreases. Furthermore, the Shared PTO system has a performance advantage over the Multi PTO system at shorter wave periods. Conversely, as wave periods increase, the performance shifts in favor of the Multi PTO system. The peak operational value for generator speed varies with changing wave conditions, demonstrating that this parameter should not be fixed but dynamically change based on the sea state.

#### 4.1.5. Highlights of the parametric analysis

The insights from this parametric analysis underline the complexity of designing the PTO of large WEC arrays that can adapt across various wave conditions. It has been established that the diameter of the hydraulic pistons, the hydraulic motor displacement, and the generator speed significantly impact the efficiency of power conversion and

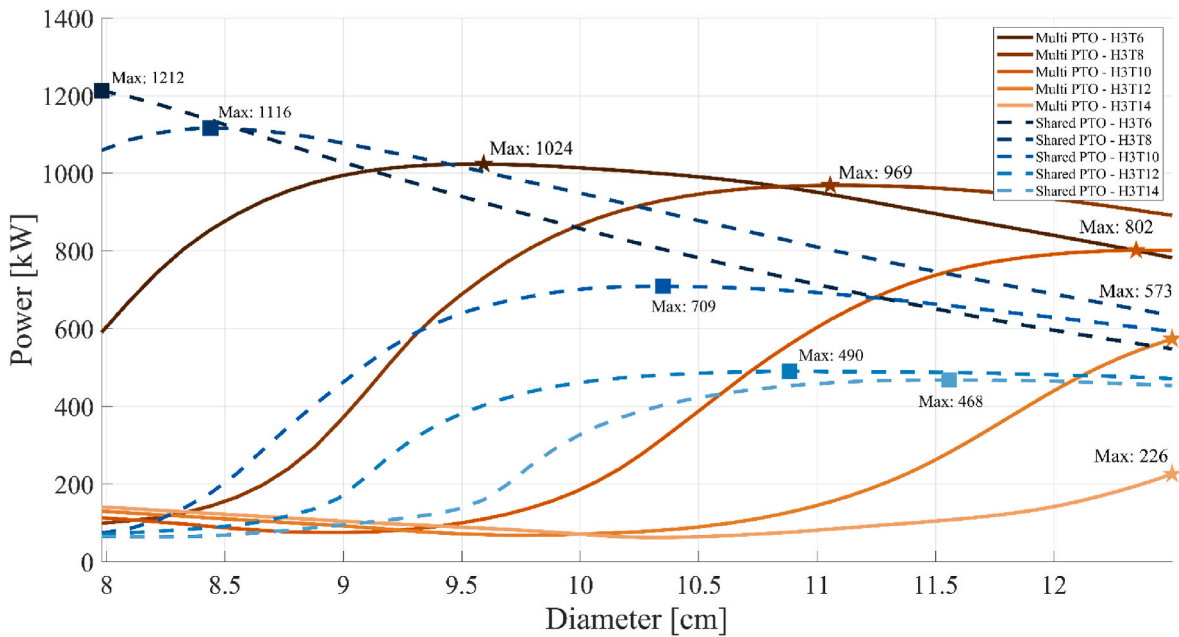


Fig. 8. Effect of hydraulic piston diameter  $D_p$  on the power generated by the WEC array for five different wave periods (6 s, 8 s, 10 s, 12 s, and 14 s) for both Multi PTO and Shared PTO V1 systems. Maximum power outputs are indicated for each scenario.

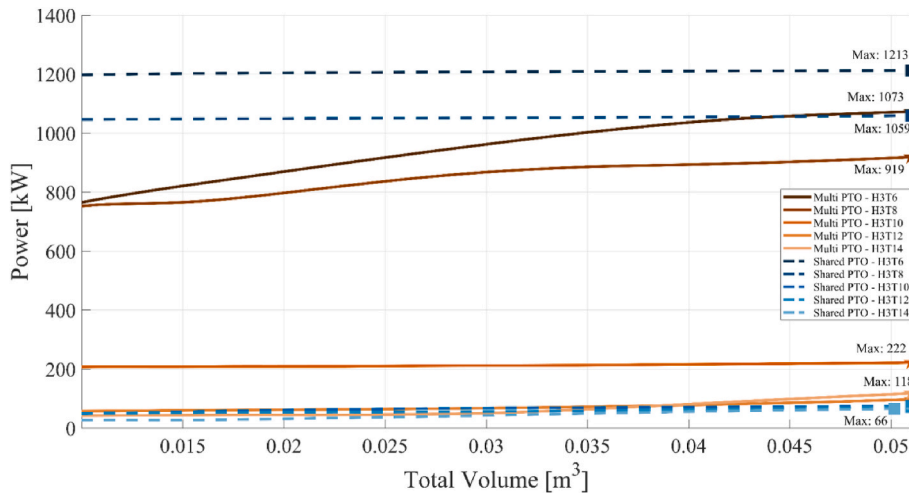


Fig. 9. Effect of high-pressure accumulator volume on the generated power from the WEC array for five different wave periods (6 s, 8 s, 10 s, 12 s, and 14 s) for both Multi PTO and Shared PTO V1 systems. Maximum power outputs are indicated for each scenario.

therefore require precise optimization due to their complex dependence on wave conditions. As a result, these variables have been identified as candidates for further refinement through a genetic algorithm.

Conversely, the initial gas volume in the high-pressure accumulator and its pre-charge pressure demonstrated a consistent trend where maximum values consistently yield the highest power output. This finding indicates that these parameters do not require variable adjustment and should be maintained at their upper limits to ensure maximum energy extraction. This approach simplifies the system’s operational requirements and enhances its overall efficiency by eliminating the need for ongoing adjustments. Thus, the study showcases how to prioritize the adaptability in critical variables while stabilizing those with uniform optimal settings.

It is important to note that the system generates maximum power at smaller wave periods (6–8 s) due to resonance effects. The hydraulic PTO system is tuned to respond optimally to higher wave frequencies, where buoy oscillations are more frequent. As the wave period increases,

the system’s efficiency decreases because the slower buoy movement causes a mismatch between the wave input and the system’s ability to convert that energy into power. This observation is common across wave energy converters, where resonance plays a critical role in power optimization [50].

## 4.2. Optimization results

### 4.2.1. Introduction

Upon optimizing the Multi and Shared PTO systems for various wave conditions, significant insights are collected. The optimization covers a comprehensive spectrum of regular wave scenarios: wave heights from 0.5 – 4 m at 0.5 m intervals, and wave periods from 4 – 14 s at 1 s increments, leading to a total of 88 distinct conditions. The key variables, namely the diameter of the hydraulic piston, the hydraulic motor displacement, and the generator speed were optimized using a genetic algorithm within the ranges specified by the manufacturers, as shown in

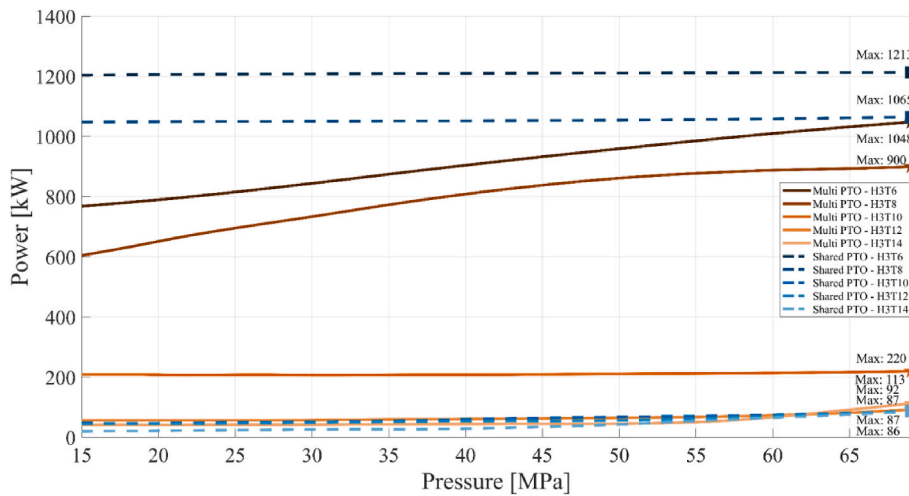


Fig. 10. Effect of pre-charge pressure in the accumulator on the generated power from the WEC array for five different wave periods (6 s, 8 s, 10 s, 12 s, and 14 s) for both Multi PTO and Shared PTO V1 systems. Maximum power outputs are indicated for each scenario.

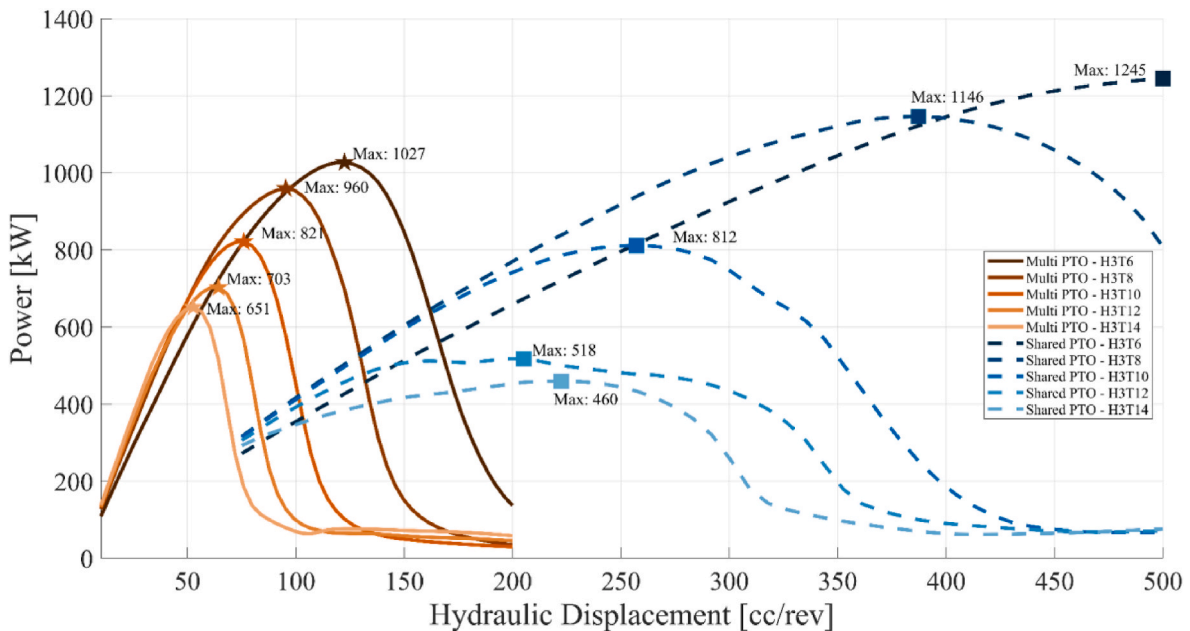


Fig. 11. Effect of the hydraulic motor displacement on the generated power from the WEC array for five different wave periods (6 s, 8 s, 10 s, 12 s, and 14 s) for both Multi PTO and Shared PTO V1 systems. Maximum power outputs are indicated for each scenario.

Table 3.

In this study, power matrices are employed to present the performance of the PTO systems under various regular wave conditions. While power matrices are typically used for irregular sea states, their application here provides a structured and clear visualization of how different wave heights and periods impact power output. This approach allows for a systematic evaluation and comparison of the PTO designs, serving as a foundational analysis before extending to more complex irregular wave conditions [38].

Figs. 13–16 illustrate the power matrices of all the PTO systems along with the percentage difference in power between each version of the Shared PTOs and the Multi PTO case, which is used as a reference configuration. The percentage difference offers insights into the relative performance between all the PTOs of the array, using the following equation:

$$\%diff = \frac{P_{Shared\ PTO\ Vx} - P_{Multi\ PTO}}{P_{Multi\ PTO}} \times 100. \quad (10)$$

#### 4.2.2. Performance of the multi PTO system

The power matrix for the Multi PTO system in Fig. 13 demonstrates that this configuration achieves its optimal performance at higher wave heights (3.5 – 4 m) and moderate wave periods (5 – 8 s), with peak power outputs reaching approximately 1.3 MW. Qualitatively analyzing these results, the trend is similar to what was previously observed for the Ocean Grazer 3.0 case, with a different PTO [40]. As wave periods extend beyond 9 s or below 5 s, the power output declines even at higher wave heights. At lower wave heights (0.5 – 2 m), the maximum power output remains consistently low, i.e.  $\leq 0.5$  MW. These findings indicate that the Multi PTO system performs best under specific wave conditions characterized by moderate to high wave heights and periods, but its power extraction drops significantly outside these conditions.

#### 4.2.3. Performance of the shared PTO V1

The Shared PTO V1 configuration shows improved performance over the Multi PTO system, particularly at larger wave heights (3.5 – 4 m)

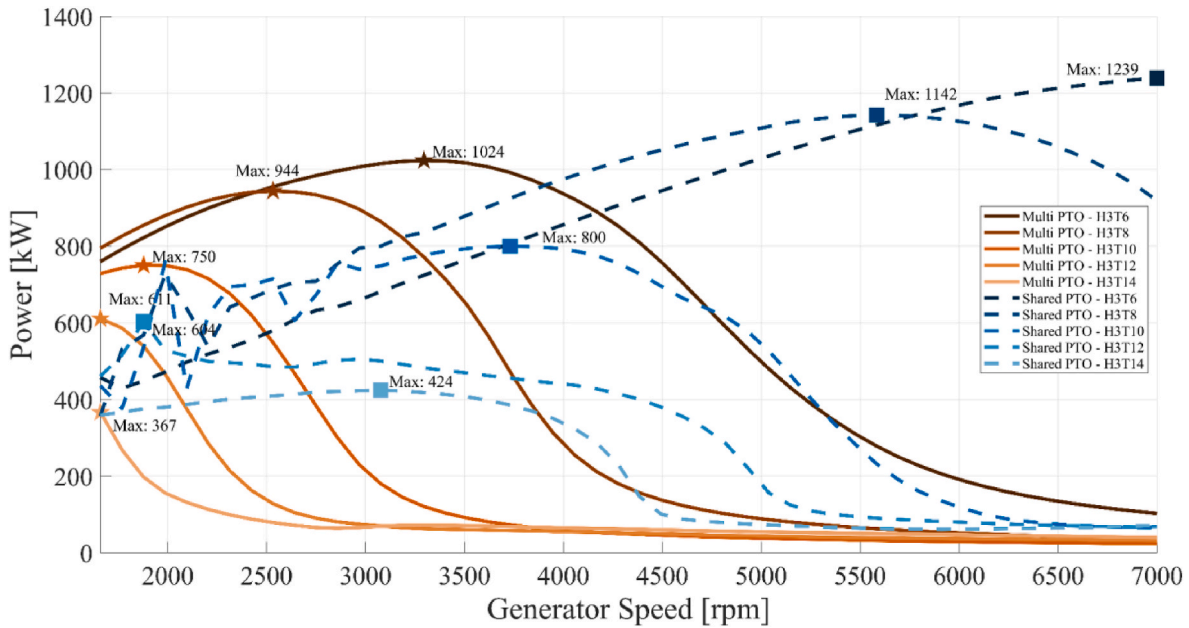


Fig. 12. Effect of the reference speed of the electric generator on the generated power from the WEC array for five different wave periods (6 s, 8 s, 10 s, 12 s, and 14 s) for both Multi PTO and Shared PTO V1 systems. Maximum power outputs are indicated for each scenario.

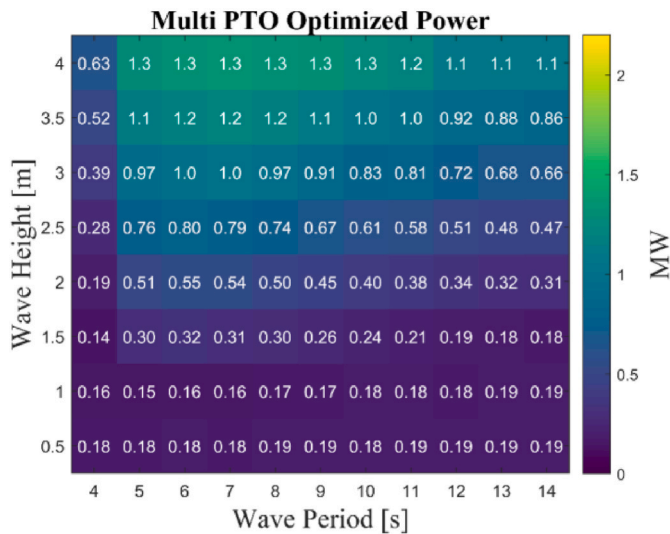


Fig. 13. Power matrix of the Multi PTO WEC array system for regular wave conditions.

and moderate wave periods (5 – 8 s), achieving peak power outputs up to 1.9 MW (Fig. 14 a). The power output decreases with wave periods extending beyond 9s or below 5s, although the shared PTO system maintains relatively higher performance within this range. At smaller wave heights, the power output is comparable to the Multi PTO system, with maximum output  $\leq 0.5$  MW. The percentage difference power matrix in Fig. 14 b indicates that the Shared PTO V1 system outperforms the Multi PTO system by up to  $\approx 45\%$  under specific wave conditions, i. e. wave heights 2.5 – 4 m and wave periods 5 – 9 s. However, outside these optimal conditions, the Multi PTO system generally exhibits better performance, with the Shared PTO V1 system producing 10– 30% less power. The superior performance of the Shared PTO can be attributed to the efficient energy extraction facilitated by the centralized PTO configuration, which benefits from more effective energy transfer.

#### 4.2.4. Performance of the shared PTO V2

The Shared PTO V2 also shows an enhancement in performance compared to both the Multi PTO and Shared PTO V1 systems, particularly at larger wave heights and moderate wave periods. This configuration achieves peak power outputs up to 2.1 MW (Fig. 15 a). However, the power output decrease at larger wave periods and shorter wave heights is more pronounced compared to Shared PTO V1. Fig. 15 b shows that the Shared PTO V2 significantly outperforms both the Multi PTO and Shared PTO V1 systems at larger wave heights and moderate wave periods, with improvements up to 55%. However, for shorter wave heights, it significantly underperforms with a notable decrease in power output (up to 83% less power). Compared to Shared PTO V1, Shared PTO V2 offers better performance at peak conditions but has a steeper decline in less favorable conditions.

#### 4.2.5. Performance of the shared PTO V3

The Shared PTO V3 exhibits mixed results. It achieves peak power outputs up to 1.8 MW at larger wave heights and moderate wave periods as shown in Fig. 16 a. However, this configuration underperforms at moderate wave heights and larger wave periods compared to both the Multi PTO and other Shared PTO configurations. Fig. 16 b indicates that the Shared PTO V3 outperforms the Multi PTO system by up to 81% at short wave heights (0.5 – 1.5 m) and across the whole frequency range. However, for larger wave periods and heights, the performance is less favorable, showing a decrease in power output (up to 16% less power). Compared to the Shared PTO V1 and V2, the Shared PTO V3 offers superior performance at short wave heights but falls short at larger wave heights and larger periods.

#### 4.2.6. Comparative analysis

Depending on the most prevalent wave conditions at the deployment site, a different configuration of the accumulators should be selected to maximize efficiency in dense WEC array configurations. This research underlines the importance of strategically distributing the accumulators across the WEC array to achieve maximum power performance. For sites with predominantly large wave heights and moderate periods, Shared PTO V1 offers the best overall performance while, for low-energy environments, Shared PTO V3 offers the best efficiency.

This research highlights the critical role of accumulator distribution

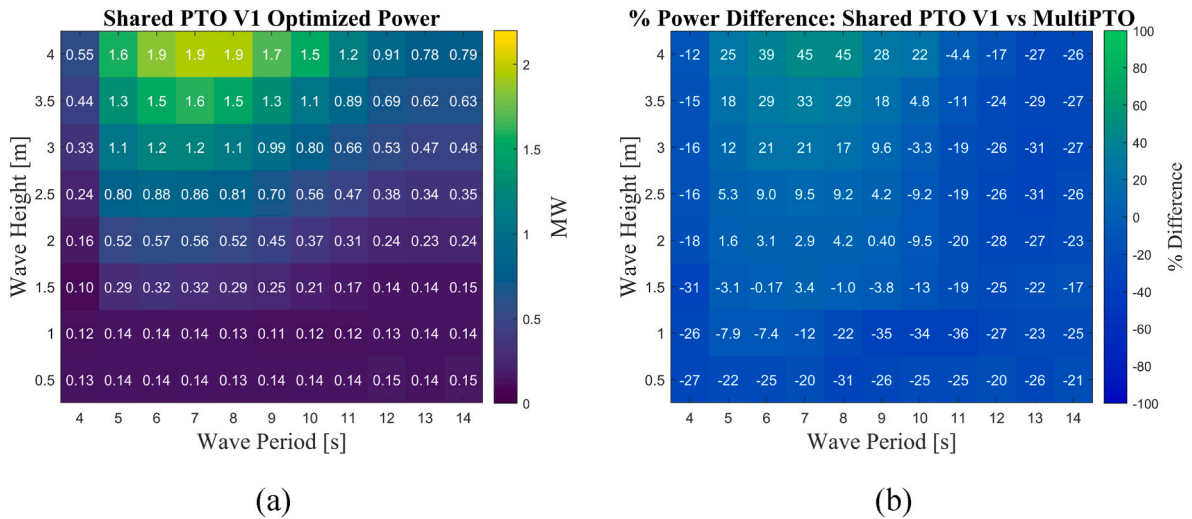


Fig. 14. Power matrix of the Shared PTO V1 for regular wave conditions (left) and the percentage difference [%] in power with respect to the Multi PTO (right).

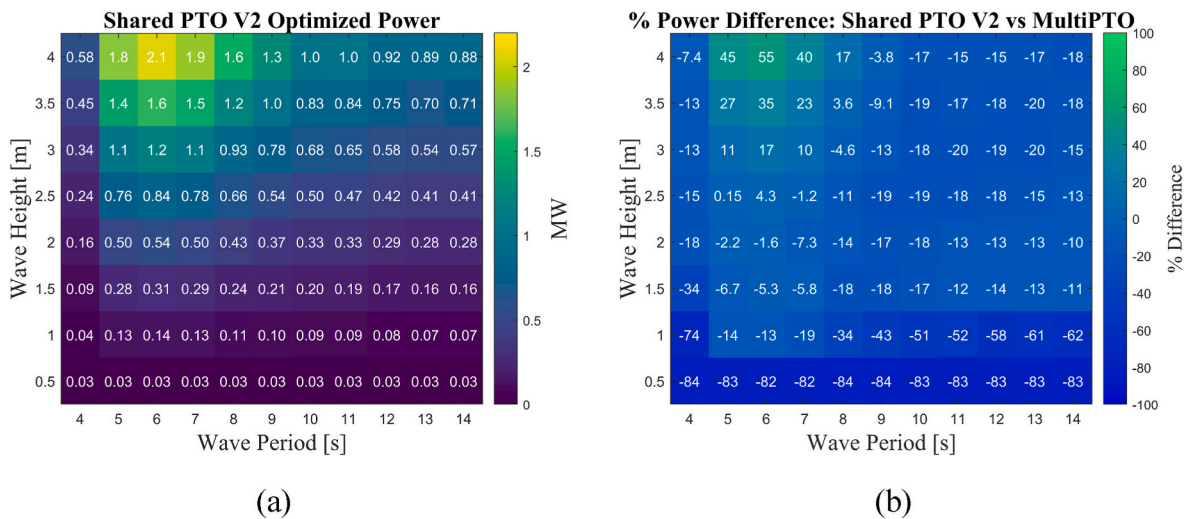


Fig. 15. Power matrix of the Shared PTO V2 for regular wave conditions (left) and the percentage difference [%] relative to the Multi PTO (right).

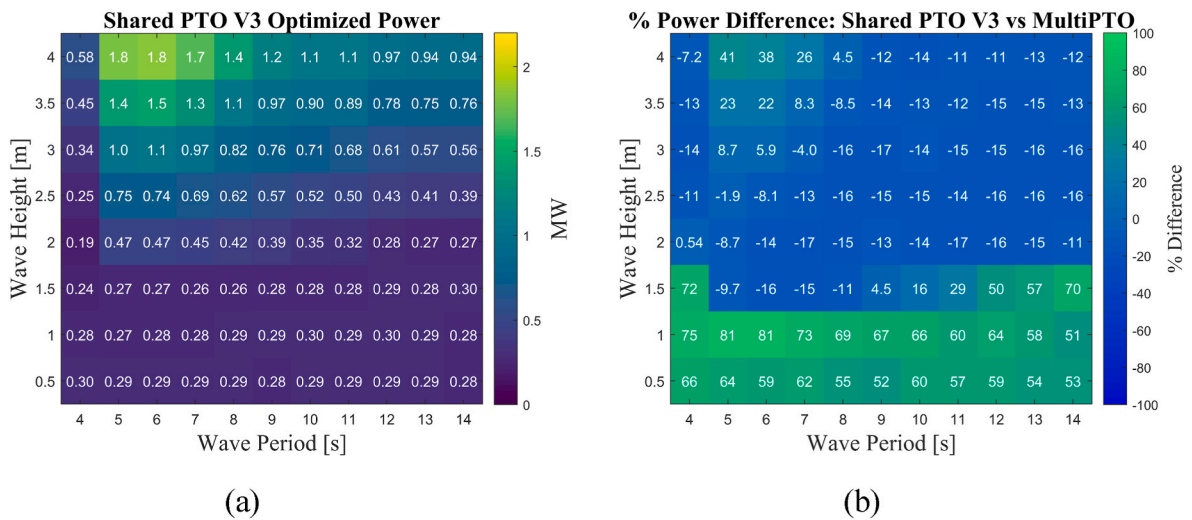


Fig. 16. Power matrix of the Shared PTO V3 for regular wave conditions (left) and the percentage difference [%] relative to the Multi PTO (right).

in enhancing the performance of WEC systems and that the optimal PTO configuration is highly dependent on the specific wave conditions at the deployment site, and careful consideration of these conditions can lead to significant improvements in power extraction efficiency. In addition to that, the reduced complexity and potential cost savings of a shared PTO system enhance its attractiveness as a viable solution for wave energy conversion in dense WEC array configurations. These centralized approaches not only reduce the number of hydraulic and electrical components but also simplify the maintenance and operational control. These factors contribute to lower capital and operational expenditures, making a Shared PTO system a more compelling choice for large-scale implementation, especially in environments where it achieves comparable or superior power output to the multi PTO system.

## 5. Conclusions

In the present work, different hydraulic PTOs of a dense WEC array were analyzed and optimized to understand the dynamics of the system under regular wave conditions. First, the influence of the most important parameters of the hydraulic PTO were analyzed under different wave conditions in a multi- and shared-PTO configuration. The key findings of this analysis are:

- **Maximizing Pre-Charge Pressure and Volume:** The pre-charge pressure and gas volume in the high-pressure accumulator should be set to their maximum possible values to ensure optimal power extraction.
- **Optimization of Key Parameters:** The diameter of the hydraulic pistons, the hydraulic motor displacement, and the speed of the electric generator should be optimized for specific wave conditions. Furthermore, these values vary depending on how the accumulator volume is distributed across the floaters of the WEC array.

The study analyzed different strategies for distributing the volume of accumulators across a dense WEC array, as illustrated in Fig. 4. Four different configurations were optimized using a genetic algorithm across 88 wave conditions, revealing:

- **Multi PTO:** Each floater has its own accumulator. It performs well at large wave heights and large wave periods.
- **Shared PTO V1:** All floaters share the same accumulator. It outperforms the Multi PTO at moderate to large wave heights and moderate wave periods but underperforms under other sea states.
- **Shared PTO V2:** Divides the accumulators into two sections across the WEC array. It shows similar performance to Shared PTO V1 but significantly underperforms at small wave heights.
- **Shared PTO V3:** Each accumulator is shared among floaters with similar phase. It performs exceptionally well across most sea states and slightly underperforms at moderate to large wave heights and periods.

This research underscores the importance of optimizing accumulator allocation in dense WEC arrays for maximizing efficiency. The findings demonstrate that an increase in power output by up to 80% is possible. Future research should focus on irregular waves to further optimize the system using real-time control strategies, enhancing practical applicability and paving the way for more efficient wave energy conversion.

## CRedit authorship contribution statement

**Andreas T. Asiikkis:** Writing – original draft, Visualization, Validation, Methodology, Investigation, Formal analysis, Data curation, Conceptualization. **Dimokratis G.E. Grigoriadis:** Writing – review & editing, Supervision, Software, Resources, Project administration, Funding acquisition, Data curation, Conceptualization. **Antonis I. Vakis:** Writing – review & editing, Supervision, Software, Resources,

Project administration, Methodology, Investigation, Funding acquisition, Data curation, Conceptualization.

## Funding

This work was supported by Multimarine Services Ltd and CMMI – Cyprus Marine and Maritime Institute. CMMI was established by the CMMI/MaRITeC-X project as a “Center of Excellence in Marine and Maritime Research, Innovation and Technology Development” and has received funding from the European Union’s Horizon 2020 research and innovation program under grant agreement No. 857586; and by a matching funding from the Government of the Republic of Cyprus.

## Declaration of competing interest

The authors declare that they have no known competing financial interests or personal relationships that could have appeared to influence the work reported in this paper.

## References

- [1] National Oceanic and Atmospheric Administration, “How many oceans are there?,” National Ocean Service website. Accessed: January, 23, 2024. [Online]. Available: <https://oceanservice.noaa.gov/facts/howmanyoceans.html>.
- [2] R. Mayon, D. Ning, B. Ding, N.Y. Sergiienko, Wave energy converter systems – status and perspectives, in: D. Ning, B. Ding (Eds.), *Modelling and Optimisation of Wave Energy Converters*, first ed., CRC Press, Boca Raton, 2022 <https://doi.org/10.1201/9781003198956> ch. 1.
- [3] D. Qiao, R. Haider, J. Yan, D. Ning, B. Li, Review of Wave Energy Converter and Design of Mooring System, MDPI, Oct. 01, 2020, <https://doi.org/10.3390/su12198251>.
- [4] K. Gunn, C. Stock-Williams, Quantifying the global wave power resource, *Renew. Energy* 44 (Aug. 2012) 296–304, <https://doi.org/10.1016/j.renene.2012.01.101>.
- [5] European Marine Energy Centre, “WAVE DEVELOPERS,” EMEC website. Accessed: January, 23, 2024. [Online]. Available: <https://www.emec.org.uk/marine-energy/wave-developers/>.
- [6] IRENA, *Innovation Outlook : Ocean Energy Technologies*, International Renewable Energy Agency, Abu Dhabi, 2020.
- [7] M.H. Jahangir, S. Ghanbari Motlagh, Feasibility study of CETO wave energy converter in Iranian coastal areas to meet electrical demands (a case study), *Energy Sustain. Develop.* 70 (Oct. 2022) 272–289, <https://doi.org/10.1016/j.esd.2022.07.017>.
- [8] A.B. Sandberg, E. Klemetsen, G. Muller, A. de Andres, J. Maillet, Critical factors influencing viability of wave energy converters in off-grid luxury resorts and small utilities, *Sustainability (Switzerland)* 8 (12) (2016), <https://doi.org/10.3390/su8121274>.
- [9] R. Waters, et al., Experimental results from sea trials of an offshore wave energy system, *Appl. Phys. Lett.* 90 (3) (2007), <https://doi.org/10.1063/1.2432168>.
- [10] T. Vervaeke, V. Stratigaki, B. De Backer, K. Stockman, M. Vantorre, P. Troch, Experimental modelling of point-absorber wave energy converter arrays: a comprehensive review, identification of research gaps and design of the WECfarm setup, *J. Mar. Sci. Eng.* 10 (8) (Aug. 2022), <https://doi.org/10.3390/jmse10081062>.
- [11] Z.Y. Tay, Energy generation enhancement of arrays of point absorber wave energy converters via Moonpool’s resonance effect, *Renew. Energy* 188 (Apr. 2022) 830–848, <https://doi.org/10.1016/j.renene.2022.02.060>.
- [12] A. Bechlenberg, Y. Wei, B. Jayawardhana, A.I. Vakis, Analysis of the impact of floater interactions on the power extraction of a dense WEC array with adaptable nonlinear PTO, in: *Proceedings of the European Wave and Tidal Energy Conference*, vol. 15, Sep. 2023, <https://doi.org/10.36688/ewtec-2023-310>.
- [13] B.W. Schubert, W.S.P. Robertson, B.S. Cazzolato, M.H. Ghayesh, Linear and nonlinear hydrodynamic models for dynamics of a submerged point absorber wave energy converter, *Ocean Eng.* 197 (Feb) (2020), <https://doi.org/10.1016/j.oceaneng.2019.106828>.
- [14] B. Guo, T. Wang, S. Jin, S. Duan, K. Yang, Y. Zhao, A Review of Point Absorber Wave Energy Converters, MDPI, Oct. 01, 2022, <https://doi.org/10.3390/jmse10101534>.
- [15] D. Golbaz, et al., Ocean wave energy converters optimization: a comprehensive review on research directions [Online]. Available: <http://arxiv.org/abs/2105.07180>, May 2021.
- [16] S.A. Sirigu, et al., Techno-Economic optimisation for a wave energy converter via genetic algorithm, *J. Mar. Sci. Eng.* 8 (8) (Jul. 2020), <https://doi.org/10.3390/JMSE8070482>.
- [17] C. Sharp, B. DuPont, Wave energy converter array optimization: a genetic algorithm approach and minimum separation distance study, *Ocean Eng.* 163 (Sep. 2018) 148–156, <https://doi.org/10.1016/j.oceaneng.2018.05.071>.
- [18] A. Shadmani, M.R. Nikoo, A.H. Gandomi, M. Chen, R. Nazari, Advancements in Optimizing Wave Energy Converter Geometry Utilizing Metaheuristic Algorithms, Elsevier Ltd, Jun. 01, 2024, <https://doi.org/10.1016/j.rser.2024.114398>.

- [19] E. Amini, et al., A comparative study of metaheuristic algorithms for wave energy converter power take-off optimisation: a case study for eastern Australia, *J. Mar. Sci. Eng.* 9 (5) (2021), <https://doi.org/10.3390/jmse9050490>.
- [20] W. Ge, S. Ji, Y. Jin, S. He, H. Chen, H. Liu, Optimization of buoy shape for wave energy converter based on particle swarm algorithm, *Appl. Sci.* 14 (5) (Feb. 2024) 1889, <https://doi.org/10.3390/app14051889>.
- [21] X. Ke, W. Liang, Optimization of energy conversion efficiency of wave energy device based on particle swarm optimization algorithm, in: 2023 IEEE International Conference on Sensors, Electronics and Computer Engineering, ICSECE 2023, Institute of Electrical and Electronics Engineers Inc., 2023, pp. 522–530, <https://doi.org/10.1109/ICSECE58870.2023.10263335>.
- [22] E. Amini, et al., Optimization of hydraulic power take-off system settings for point absorber wave energy converter, *Renew. Energy* 194 (Jul. 2022) 938–954, <https://doi.org/10.1016/j.renene.2022.05.164>.
- [23] J.A. Leon-Quiroga, G. Bacelli, D.D. Forbush, S.J. Spencer, R.G. Coe, An efficient and effective WEC power take-off system, *IEEE Trans. Sustain. Energy* 14 (3) (Jul. 2023) 1526–1539, <https://doi.org/10.1109/TSTE.2023.3237125>.
- [24] V.V.S. Sricharan, S. Chandrasekaran, Time-domain analysis of a bean-shaped multi-body floating wave energy converter with a hydraulic power take-off using WEC-Sim, *Energy* 223 (May 2021), <https://doi.org/10.1016/j.energy.2021.119985>.
- [25] M.A. Jusoh, M.Z. Ibrahim, M.Z. Daud, Z.M. Yusop, A. Albani, An estimation of hydraulic power take-off unit parameters for wave energy converter device using non-evolutionary nlpql and evolutionary ga approaches, *Energies (Basel)* 14 (1) (Jan. 2021), <https://doi.org/10.3390/en14010079>.
- [26] K.T. Waskito, A. GERALDI, A.C. Ichi, Yanuar, G.P. Rahardjo, I. Al Ghifari, Design of hydraulic power take-off systems unit parameters for multi-point absorbers wave energy converter, *Energy Reports* 11 (Jun. 2024) 115–127, <https://doi.org/10.1016/j.egy.2023.11.042>.
- [27] C.J. Cargo, A.R. Plummer, A.J. Hillis, M. Schlotter, Determination of optimal parameters for a hydraulic power take-off unit of a wave energy converter in regular waves, *Proc. Inst. Mech. Eng. A J. Power Energy* 226 (1) (2012) 98–111, <https://doi.org/10.1177/0957650911407818>.
- [28] G. He, et al., Review on research approaches for multi-point absorber wave energy converters, *Renew. Energy* 218 (Dec) (2023), <https://doi.org/10.1016/j.renene.2023.119237>.
- [29] Y. Wei, et al., Frequency-domain hydrodynamic modelling of dense and sparse arrays of wave energy converters, *Renew. Energy* 135 (May 2019) 775–788, <https://doi.org/10.1016/j.renene.2018.12.022>.
- [30] Y. Wei, A. Bechlenberg, B. Jayawardhana, A.I. Vakis, Modelling of a wave energy converter array with non-linear power take-off using a mixed time-domain/frequency-domain method, *IET Renew. Power Gener.* 15 (14) (Oct. 2021) 3220–3231, <https://doi.org/10.1049/rpg2.12231>.
- [31] Y. Wei, A. Bechlenberg, M. van Rooij, B. Jayawardhana, A.I. Vakis, Modelling of a wave energy converter array with a nonlinear power take-off system in the frequency domain, *Appl. Ocean Res.* 90 (Sep) (2019), <https://doi.org/10.1016/j.apor.2019.05.009>.
- [32] R.M. Nienhuis, M. van Rooij, W.A. Prins, B. Jayawardhana, A.I. Vakis, Investigating the efficiency of a novel offshore pumped hydro energy storage system: experimental study on a scale prototype, *J. Energy Storage* 74 (Dec. 2023), <https://doi.org/10.1016/j.est.2023.109374>.
- [33] M. Ancellin, F. Dias, Capytaine: a Python-based linear potential flow solver, *J. Open Source Softw.* 4 (36) (Apr. 2019) 1341, <https://doi.org/10.21105/joss.01341>.
- [34] D. Ogden, et al., Review of WEC-sim development and applications, *Int. Marine Energy J.* 5 (3) (Dec. 2022) 293–303, <https://doi.org/10.36688/imej.5.293-303>.
- [35] Matthieu Ancellin, “Capytaine,” Capytaine: a Python-based linear potential flow BEM solver [Online]. Available: <https://capytaine.github.io/>. (Accessed 10 July 2024).
- [36] National Renewable Energy Laboratory and National Technology & Engineering Solutions of Sandia, “WEC-sim,” WEC-Sim (Wave Energy Converter Simulator). Accessed: July. 10, 2024. [Online]. Available: [wec-sim.github.io/WEC-Sim](http://wec-sim.github.io/WEC-Sim).
- [37] R. So, A. Simmons, T. Brekken, K. Ruehl, C. Michelen, Development of pto-sim: a power performance module for the open-source wave energy converter code wec-sim [Online]. Available: <http://proceedings.asmedigitalcollection.asme.org/pdfaccess.ashx?url=/data/conferences/asmep/86142/>, 2015.
- [38] A. Babarit, G. Delhommeau, Theoretical and numerical aspects of the open source BEM solver NEMOH, in: 11th European Wave and Tidal Energy Conference (EWTEC2015), Nantes, France: EWTEC2015, Sep. 2015.
- [39] The MathWorks Inc, How the genetic algorithm works [Online]. Available: <https://www.mathworks.com/help/gads/how-the-genetic-algorithm-works.html>. (Accessed 10 July 2024).
- [40] A. Bechlenberg, Y. Wei, B. Jayawardhana, A.I. Vakis, Analysing the influence of power take-off adaptability on the power extraction of dense wave energy converter arrays, *Renew. Energy* 211 (Jul. 2023) 1–12, <https://doi.org/10.1016/j.renene.2023.04.076>.
- [41] N. Tom, Review of wave energy converter power take-off systems, testing practices, and evaluation metrics, in: *Energy*, vol. 6, American Society of Mechanical Engineers, Oct. 2022, <https://doi.org/10.1115/IMECE2022-94077>.
- [42] PARKER HANNIFIN CORP, Parker [Online]. Available: <https://www.parker.com/us/en/home.html>, 2024. (Accessed 10 June 2024).
- [43] M.A. Jusoh, et al., Parameters estimation of hydraulic power take-off system for wave energy conversion system using genetic algorithm, in: IOP Conference Series: Earth and Environmental Science, Institute of Physics Publishing, Apr. 2020, <https://doi.org/10.1088/1755-1315/463/1/012129>.
- [44] Y. Xuhui, et al., A novel nonlinear state space model for the hydraulic power take-off of a wave energy converter, *Energy* 180 (Aug. 2019) 465–479, <https://doi.org/10.1016/j.energy.2019.05.095>.
- [45] PARKER HANNIFIN INDUSTRIAL (M) SDN.BHD, 16MPa double acting hydraulic cylinder model:160H-1 [Online]. Available: <https://ph.parker.com/my/en/product-t-list/for-16-mpa-double-acting-hydraulic-cylinder-rod-disposed-of-shape-model-160-h-1>. (Accessed 19 January 2024).
- [46] PARKER HANNIFIN INDUSTRIAL (M) SDN.BHD, Bladder accumulator - high pressure (EHV) - (europe) [Online]. Available: <https://ph.parker.com/my/en/product-list/bladder-accumulator-high-pressure-ehv>. (Accessed 19 January 2024).
- [47] Bladder Accumulator - Low Pressure (EBV Series) - (Europe), Bladder accumulator - low pressure (EBV series) - (Europe) [Online]. Available: <https://ph.parker.com/my/en/product/low-pressure-bladder-accumulator-ebv/10910401125>. (Accessed 19 January 2024).
- [48] PARKER HANNIFIN INDUSTRIAL (M) SDN.BHD, High Torque radial piston motors - series MR [Online]. Available: <https://ph.parker.com/my/en/product-list/high-torque-radial-piston-motors-series-mr>. (Accessed 19 January 2024).
- [49] PARKER HANNIFIN INDUSTRIAL (M) SDN.BHD, Frameless spindle motors - HKW310\_500HBY [Online]. Available: <https://ph.parker.com/my/en/product-list/frameless-spindle-motors-hkw-series>. (Accessed 19 January 2024).
- [50] T. Aderinto, H. Li, Review on power performance and efficiency of wave energy converters, *Energies (Basel)* 12 (22) (Nov. 2019) 4329, <https://doi.org/10.3390/en12224329>.